Intravascular innate immune cells reprogrammed via intravenous nanoparticles to promote functional recovery after spinal cord injury

Jonghyuck Park[a], Yining Zhang[b], Eiji Saito[a], Steve J. Gurczynski[c], Bethany B. Moore[c], Brian J. Cummings[d], Aileen J. Anderson[d], and Lonnie D. Shea[a,b,1]

[a]Department of Biomedical Engineering, University of Michigan, Ann Arbor, MI 48105; [b]Department of Chemical Engineering, University of Michigan, Ann Arbor, MI 48105; [c]Department of Microbiology and Immunology, University of Michigan, Ann Arbor, MI 48105; and [d]Department of Anatomy and Neurobiology, University of California, Irvine, CA 92697

Edited by Kristi S. Anseth, University of Colorado Boulder, Boulder, CO, and approved June 11, 2019 (received for review November 27, 2018)

Traumatic primary spinal cord injury (SCI) results in paralysis below the level of injury and is associated with infiltration of hematogenous innate immune cells into the injured cord. Methylprednisolone has been applied to reduce inflammation following SCI, yet was discontinued due to an unfavorable risk-benefit ratio associated with off-target effects. In this study, i.v. administered poly(lactide-coglycolide) nanoparticles were internalized by circulating monocytes and neutrophils, reprogramming these cells based on their physicochemical properties and not by an active pharmaceutical ingredient, to exhibit altered biodistribution, gene expression, and function. Approximately 80% of nanoparticle-positive immune cells were observed within the injury, and, additionally, the overall accumulation of innate immune cells at the injury was reduced 4-fold, coinciding with down-regulated expression of proinflammatory factors and increased expression of antiinflammatory and proregenerative genes. Furthermore, nanoparticle administration induced macrophage polarization toward proregenerative phenotypes at the injury and markedly reduced both fibrotic and gliotic scarring 3-fold. Moreover, nanoparticle administration with the implanted multichannel bridge led to increased numbers of regenerating axons, increased myelination with about 40% of axons myelinated, and an enhanced locomotor function (score of 6 versus 3 for control group). These data demonstrate that nanoparticles provide a platform that limits acute inflammation and tissue destruction, at a favorable risk-benefit ratio, leading to a proregenerative microenvironment that supports regeneration and functional recovery. These particles may have applications to trauma and potentially other inflammatory diseases.

spinal cord injury | nerve regeneration | nanomedicine | immunoengineering

Traumatic spinal cord injury (SCI) results in an initial injury, followed by secondary events that can last from hours to weeks leading to permanent loss of function (1–3). Inflammatory responses are initiated in part by the rapid influx of immune cells, including inflammatory monocytes and neutrophils, via a broken blood-spinal cord barrier. These cells infiltrate the injury site within hours and secrete proinflammatory cytokines, reactive oxygen species, and nitric oxide, all of which can contribute to additional neuronal cell death, axonal demyelination, and functional deficits following SCI (4–7). Critically, while glucocorticoids such as methylprednisolone were once the standard of care for acute SCI due to their antiinflammatory properties, these agents are also associated with unfavorable side effects, such as sepsis, gastrointestinal bleeding, and thromboembolism (8, 9), indicating that improved methods are needed. Systemic depletion of neutrophils or monocytes has either not altered or has had a small effect on SCI outcome (10). Because monocytes and neutrophils are necessary for wound healing and tissue regeneration after injury, reprogramming the immune response could be a more effective strategy to minimize loss of function and enable repair.

We have previously demonstrated that 500-nm-diameter poly(lactide-coglycolide) (PLG)-based nanoparticles (NPs) carrying a negative zeta potential distract circulating immune cells such as inflammatory monocytes and neutrophils away from the injury site (11, 12). i.v.-administered NPs reduced pathological symptoms and produced a therapeutic benefit in inflammation-mediated diseases on the central nervous system (CNS) including West Nile virus, encephalitis, and experimental autoimmune encephalomyelitis (11–13). Highly negatively charged NPs are thought to bind to the scavenger receptor on circulating immune cells, effectively reprogramming them to influence their trafficking to the spleen and, thus, indirectly attenuate the immune pathology at the inflamed area (12, 13). In SCI, recent studies demonstrate that hematogenous-infiltrating immune cells are predominantly responsible for secondary axonal dieback, suggesting that reducing hematogenous immune cell infiltration at early time points may indirectly reduce tissue degeneration by attenuating the inflammation-mediated secondary events (14, 15). Reprogramming immune cells to accumulate at the injury and assume proregenerative phenotypes may provide a

Significance

Inflammatory responses, such as those following spinal cord injury (SCI), lead to extensive tissue damage that impairs function. Here, we present nanoparticles that target circulating immune cells acutely, with nanoparticles reprogramming the immune cell response. The polymeric nanoparticles are formed without an active pharmaceutical ingredient that can have off-target effects, and internalization redirects some immune cells to the spleen, with modest numbers at the SCI. Following intravenous delivery, immune cell infiltration is reduced, correlating with decreased tissue degeneration. Furthermore, the SCI develops into a permissive microenvironment characterized by proregenerative immune cell phenotypes, expression of regeneration associated genes, increased axons and myelination, and a substantially improved functional recovery. These nanoparticles may be applied to numerous inflammatory diseases.

Author contributions: J.P. and L.D.S. designed research; J.P., Y.Z., S.J.G., and B.B.M. performed research; J.P., B.J.C., A.J.A., and L.D.S. analyzed data; and J.P., Y.Z., E.S., B.J.C., A.J.A., and L.D.S. wrote the paper.

The authors declare no conflict of interest.

This article is a PNAS Direct Submission.

[1]To whom correspondence may be addressed. Email: ldshea@umich.edu.

This article contains supporting information online at www.pnas.org/lookup/suppl/doi:10.1073/pnas.1820276116/-/DCSupplemental.

Published online July 8, 2019.

means to directly modulate the injury environment to promote regeneration.

Herein, we investigate NPs that reprogram inflammatory cells intravascularly to obtain a fraction that home to the injury and modulate the microenvironment, resulting in enhanced regeneration and functional recovery after SCI. NPs (500 nm diameter, zeta potential < −30 mV) were administered i.v. daily for 7 d immediately after SCI. A lateral hemisection SCI model was employed, with bridge implantation employed in all studies as a means to define a region in which spared axons can be distinguished from regenerating axons (*SI Appendix*, Fig. S1). We investigate the biodistribution of NPs among tissues by fluorescence imaging and, subsequently, within the spinal cord. Inflammatory responses were characterized histologically and through gene expression analysis. Regeneration following NP treatment was assessed through the number of axons, the presence of serotonergic axons, and myelination of axons with locomotor functional testing performed. The administration of NPs targets innate immune cells to reprogram their function, which represents a strategy for neuroprotection and neuroregeneration after SCI.

Results

NP Internalization and Immune Cell Sequestration. In vivo images were acquired to investigate the biodistribution of NPs. Initially, NPs (1 mg, Cy5.5-conjugated [NPs-Cy5.5]) were administered i.v. on a daily basis for 7 d starting the day of injury (Fig. 1*A*). The spinal cord, spleen, and liver were collected for analysis at day 1, 4, and 8 after injection from all conditions (day 7, 10, and 14 after SCI) (Fig. 1*B* and *SI Appendix*, Figs. S2 and S3). In both SCI and sham groups, the greatest fluorescence intensity from NPs was observed in liver. However, fluorescence associated with NPs was also observed in the spinal cord and spleen (Fig. 1*C*). Radiant efficiency levels associated with NPs-Cy5.5 in the spinal cord were approximately 3-fold greater in the SCI group compared with the sham group; in contrast, in the spleen and liver,

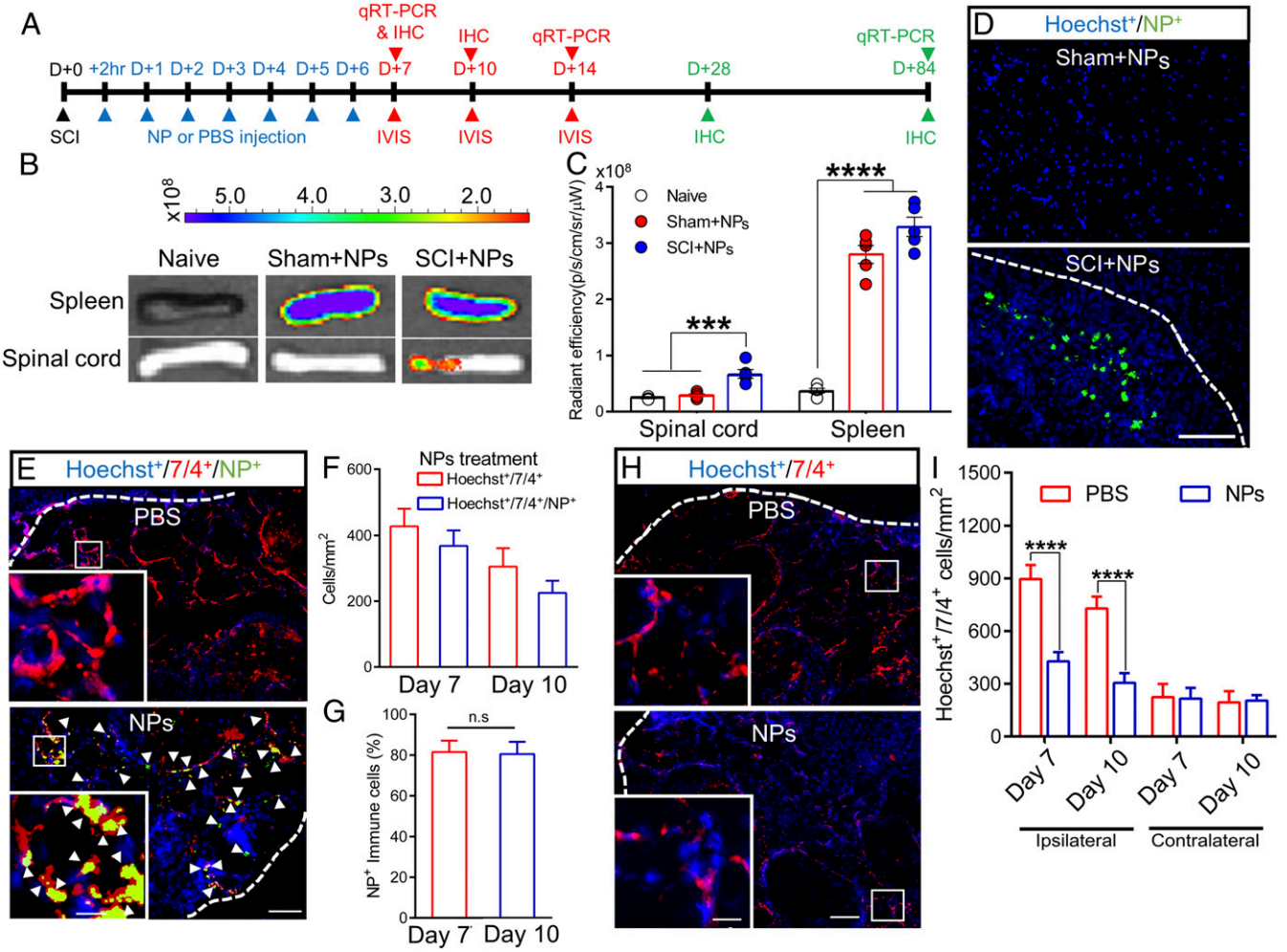

Fig. 1. In vivo biodistribution analysis and internalization of NPs. (*A*) Experimental timeline in this study. (*B*) In vivo imaging system images from the spinal cord and spleen were acquired at day 1 after injection. (*C*) The fluorescence intensity was quantified in organs from all conditions. (*D*) NPs-Cy5.5 were observed within the injury from SCI group at day 7 after SCI. The white line indicates implanted bridge area within the spinal cord. (*E*) Spinal cord sections were labeled with anti-7/4 and Hoechst at day 7 after SCI. NPs-Cy5.5 colocalized with inflammatory monocytes/neutrophils (yellow) within SCI in the NP group. (*Inset*) High-magnification image of Hoechst$^+$/7/4$^+$/NP$^+$ within bridge area (white arrowheads). (*F* and *G*) The number of Hoechst$^+$/7/4$^+$/NP$^+$ and Hoechst$^+$/7/4$^+$ cells within bridge area from the NPs group (*F*) and percentage of NPs-Cy5.5 expressing immune cells (*G*) at day 7 and 10 after SCI. More than 80% of immune cells were colocalized with NPs-Cy5.5 within SCI. (*H*) 7/4$^+$ immune cells distribution from both groups at day 10 after SCI. (*I*) Number of accumulated immune cells was quantified at day 7 (*E*) and 10 (*H*) after SCI from both conditions from ipsilateral and contralateral sides. A 2-way ANOVA with Tukey's post hoc test for the multiple comparisons or unpaired *t* test (2-tailed) was performed (*G*), where ***$P < 0.001$ and ****$P < 0.0001$ compared with PBS group, mean ± SD, $n = 5$ per group and time point. n.s., not significant. (Scale bars: *D*, 200 μm; *E*, 50 μm; *H*, 100 μm.)

no differences were observed between sham and SCI groups. Subsequently, fluorescence levels gradually decreased in all sites over time (*SI Appendix*, Figs. S2 and S3). At day 4 after injection (day 10 after SCI), the fluorescence associated with NPs-Cy5.5 was substantially decreased in the spleen and liver, yet no significant differences were observed in the spinal cord compared with those at day 1 postinjection. However, the fluorescence associated with NPs-Cy5.5 was decreased in all organs as in the naïve group at day 8 after injection.

Next, the distribution of particles within the spinal cord and cell types with internalized particles were investigated. Cy5.5 fluorescence was observed within the bridge area after SCI (Fig. 1*D*). In addition, immunofluorescence data indicated that about 80% of NPs-Cy5.5 were colocalized with 7/4 $(Ly\text{-}6B.2)^+$ inflammatory monocytes/neutrophils within the bridge (Fig. 1 *E*–*G*). Anti-7/4 was selected as a marker for inflammatory monocytes/neutrophils, since the 7/4 antigen is present on the cell surface of both inflammatory monocytes and neutrophils (16). We subsequently investigated inflammation within the spinal cord, specifically focusing on the accumulation of inflammatory monocytes/neutrophils and gene expression associated with immune cells. At days 7 and 10 after SCI, $7/4^+$ cell numbers in the injury with NP administration were significantly reduced relative to control conditions and no differences were observed in contralateral spinal cord (Fig. 1 *H* and *I* and *SI Appendix*, Fig. S4). Gene expression levels for neutrophils (CD11b and Ly6G) and inflammatory monocytes (CCR2 and Ly6C) were investigated in the spinal cord and spleen at day 7 after SCI. The data indicated that NP administration significantly decreased the expression of genes associated with neutrophils and inflammatory monocytes within the spinal cord compared with the phosphate-buffered saline (PBS) group (*SI Appendix*, Fig. S5*A*). Although Ly6C gene expression level within the spleen for NP treatment trended toward greater expression compared with the PBS group, these trends were not significant. However, CD11b, Ly6G, and CCR2 expression levels in the spleen from the NP group were significantly increased relative to the PBS group (*SI Appendix*, Fig. S5*B*). In the spleen, NPs colocalized with $7/4^+$ cells (*SI Appendix*, Fig. S6) and $MARCO^+$ cells (*SI Appendix*, Fig. S7 *A*–*C*). Additionally, in vitro NP internalization assays demonstrated that addition of soluble MARCO significantly decreased NPs internalization (*SI Appendix*, Fig. S7*D*). Collectively, in agreement with previous studies (12, 13, 17), these results suggest that NP administration associates with innate immune cells such as inflammatory monocytes and neutrophils, which influence their numbers in the spleen and spinal cord. In addition, NP administration contributes to decreasing immune cells accumulation at inflamed sites.

NPs Induce Macrophage Polarization at the Injury Site. We next investigated macrophage polarization following NP treatment of SCI, as macrophages play pivotal roles in inflammatory responses after injury (14, 18) (Fig. 2). Macrophages have the potential for plasticity in their phenotype depending on their microenvironment, and although macrophage phenotypes are not binary, they have been classified as inflammatory M1 and proregenerative M2 phenotypes for ease of description (18). We have reported that M2 macrophages contribute to creating proregenerative microenvironments leading to axonal regrowth and remyelination, and locomotor recovery after SCI (19, 20). Analysis of markers for M1 and M2 macrophages in the spinal cord indicated that expression levels of the proinflammatory markers inducible nitric oxide synthase (iNOS), CD86, and monocyte chemoattractant protein-1 (MCP-1) were significantly down-regulated in the NPs compared with the PBS group from day 7. As key markers for M1 phenotypes, these factors are associated with inflammatory responses and release of proinflammatory factors, contributing to an inhibitory microenvironment at the injury (18). In contrast, levels of the M2 markers CD206 and interleukin (IL)-10 were significantly increased in the NPs relative to the PBS group. These results were maintained until day 84 after SCI (Fig. 2 *A* and *B*). In agreement with previous studies (19, 21), no difference was observed in Arginase1 (Arg1) expression between groups at day 7, yet Arg1 was significantly up-regulated following NP treatment at day 14 and 84 after SCI compared with PBS. Interestingly, expression levels of proinflammatory factors (CD86 and MCP-1) were reduced in the PBS group compared with SCI only, while antiinflammatory markers (Arg1 and CD206) were substantially increased in the PBS group compared with SCI only at day 84 after SCI, indicating a role of the bridge for limiting inflammation. Subsequently, immunofluorescence data were investigated to quantify the total number of $CD206^+$ cells

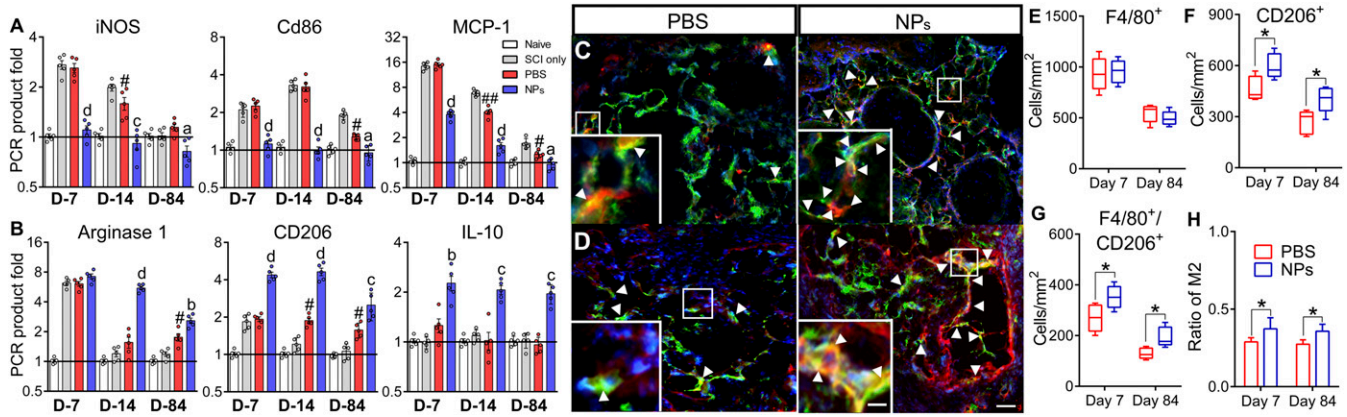

Fig. 2. Immunomodulation and macrophages polarization by NPs. (*A* and *B*) qRT-PCR data indicate modulation of selected proinflammatory (*A*) and antiinflammatory (*B*) markers at day 7, 14, and 84 after SCI by NP treatment. A 2-way ANOVA with Tukey's post hoc test for the multiple comparisons, where $^aP < 0.05$, $^bP < 0.01$, $^cP < 0.001$, and $^dP < 0.0001$, compared with PBS group and $^{\#}P < 0.05$ and $^{\#\#}P < 0.01$ relative to SCI only group, mean ± SD, $n = 5$ per group and time point. (*C* and *D*) Immunodetection of M2 ($CD206^+/F4/80^+/Hoechst^+$; red, green, and blue, respectively) macrophages (yellow), (white arrowheads) within bridge from all conditions at day 7 (*C*) and day 84 after SCI (*D*). (*Inset*) High-magnification image of M2 within bridge area. (*E*) The density of total $F4/80^+$ macrophages within the bridge. No changes were observed between groups. (*F*) The quantitative analysis of $CD206^+$ cells. NPs up-regulate the expression of $CD206^+$ cells. (*G*) The density of M2 by NPs. (*H*) The ratio of M2 to the total number of macrophages. A 2-way ANOVA with Tukey's post hoc test for the multiple comparisons, where $^*P < 0.05$ compared with PBS group, mean ± SD, $n = 5$ per group and time point. (Scale bars: *C* and *D*, 100 μm; *C* and *D Inset*, 50 μm.)

(Hoechst$^+$/CD206$^+$), macrophages (Hoechst$^+$/F4/80$^+$), and M2 macrophages (Hoechst$^+$/F4/80$^+$/CD206$^+$) at day 7 and 84 after SCI (Fig. 2 *C* and *D*). The number of CD206$^+$ cells was significantly increased in the NPs compared with PBS group (Fig. 2*F*). The density of proregenerative M2 macrophages was about 2-fold up-regulated for the NPs group at day 7 and 84 after SCI (Fig. 2*G*). Furthermore, no statistical difference was noted in the total number of infiltrated macrophages for all conditions (Fig. 2*E*) over time, thus the ratio of M2 phenotypes to the total number of macrophages was substantially up-regulated in NP group (Fig. 2*H*). Therefore, NP administration influences macrophage polarization at the SCI.

NP Treatment Decreases Scarring Formation after SCI. SCI results in formation of both fibrotic and gliotic scar tissues at the lesion epicenter; we therefore investigated the impact of the NPs on these parameters. The scar tissue acts as a mechanical barrier to axon elongation and inhibiting axonal regeneration through accumulation of inhibitory molecules as a chemical barrier (1, 2). A fibrotic scar is characterized by accumulation of fibronectin, fibroblasts, and various extracellular matrix molecules. Reactive astrocytes play prominent roles in formation of gliotic scar and act as a major impediment to axonal regeneration (2). At 4 wk after SCI, the area of fibrotic scar tissue in the NP treatment group was decreased more than 2-fold compared with PBS (Fig. 3 *A* and *B*). Similar to the level of fibronectin, the area of glial fibrillary acidic protein (GFAP) staining in the NP group was also substantially decreased 2- to 3-fold relative to the PBS group (Fig. 3 *C* and *D*). No differences were observed compared with naïve group (*SI Appendix*, Fig. S8). These data indicate that NP administration significantly decreased both fibrotic and gliotic scarring after SCI.

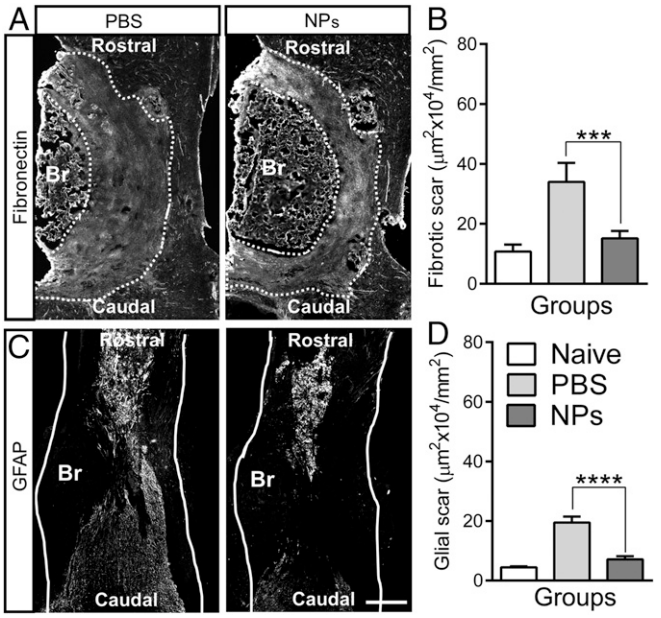

Fig. 3. NP treatment reduces the fibrotic and gliotic scarring after SCI. (*A* and *C*) Spinal cord tissues were stained with anti-fibronectin (*A*) and anti-GFAP (*C*) using longitudinal sections from 4 wk after SCI (Br, bridge); dashed line indicates the area of fibrotic scar tissue around bridge and white line indicates host spinal cord. (Scale bar: 400 μm.) (*B* and *D*) Quantification of fibrotic (*B*) and glial (*D*) scarring around implanted bridge area. No differences were observed between the naïve and NP group. The area of both fibrotic and glia scar was substantially decreased by NP treatment. A one-way ANOVA with Tukey's post hoc test for the multiple comparisons, where ***$P < 0.001$ and ****$P < 0.0001$ compared with PBS group, mean ± SD, n = 5 per group and time point.

NPs Enhance Axonal Regrowth and Remyelination within an Implanted PLG Bridge. We investigated the impact of NP treatment on axonal regrowth and myelination in the chronic (day 84 after SCI) phase of SCI (Fig. 4). Spinal cord sections were stained using neurofilament 200 (NF200), myelin basic protein (MBP), and myelin protein zero (P0). Immunofluorescence data indicated that axons were observed throughout the bridges in all conditions (Fig. 4 *A* and *B* and *SI Appendix*, Fig. S9). High magnification images showed that regenerating axons were found in bundles within the bridge (Fig. 4 *A′* and *B′*). NP administration substantially increased the number of NF200$^+$ axons relative to the PBS group (Fig. 4*C*). Similar to NF200$^+$ axons number, all myelinated axons (NF200$^+$/MBP$^+$) were increased 3-fold in response to NPs relative to PBS injection. In addition, the significantly greater number of oligodendrocyte- (NF200$^+$/MBP$^+$/P0$^-$) and Schwann cell-derived myelinated (NF200$^+$/MBP$^+$/P0$^+$) axons were observed for NP treatment relative to the PBS group. Furthermore, about 43% of the NF200$^+$ axons were myelinated in the NP condition, with ∼40% of those axons myelinated by oligodendrocytes, which were similar to those in uninjured contralateral side (Fig. 4 *D* and *E*). Collectively, these data suggest that NPs produce an environment more permissive to axonal growth and remyelination after SCI.

NPs Increase the Density of 5-Hydroxytryptamine Fibers after SCI. The presence of axons that are positive for the neurotransmitter serotonin (or 5-hydroxytryptamine [5-HT]) was assessed because these axons have been associated with recovery of function and attenuation of allodynia/hyperalgesia after SCI (22, 23). This role of 5-HT axons in function makes it a good marker for regeneration of descending tracts. Spinal cord tissues were immunostained for 5-HT at day 84 after SCI, and the densities of 5-HT fibers quantified at 3 distinct locations of the bridge: rostral, central, and caudal (Fig. 5 and *SI Appendix*, Fig. S1*C*). 5-HT fibers were identified throughout the bridge; however, about 5 to 9 times greater density of 5-HT fibers was observed with NP treatment in all 3 locations compared with PBS (Fig. 5 *A′*, *B′*, and *C*). Although data showed a trend toward greater intensity of 5-HT at rostral and central locations in contralateral side relative to NPs, no significant changes were observed between groups. These data suggest that in addition to the observation of neurofilament axons and active remyelination within the bridge, NP treatment specifically resulted in the growth of descending motor axons as assessed by density of 5-HT fibers within the bridge.

NPs Improve Locomotor Function after SCI. We next investigated the expression of regeneration-associated genes (RAGs) following NP administration in the acute and chronic SCI phase from the injured spinal cord tissue (Fig. 6 *A* and *B*). Genes were selected from neural system development (Gene Ontology [GO] accession no. GO:0007399), locomotor recovery- (GO:0007626), and chemical synaptic transmission- (GO:0007268) associated gene ontologies based on a previous study (20). Gene expression data indicated that selected genes had up-regulated expression in the the NP group for both the acute and chronic phase of SCI relative to PBS injection. Interestingly, in the chronic SCI phase, expression levels of RAGs (ChAT, Hoxd10, and Lhx5) in the PBS injection group were also statistically up-regulated relative to SCI only group, suggesting a role for the bridge alone in supporting regeneration. Subsequently, ipsilateral hindlimb locomotor recovery was assessed through the Basso Mouse Scale (BMS) before injury, at day 3, and weekly for 84 d after SCI (Fig. 6*C*). All animals exhibited normal open field locomotion before SCI (BMS;9). No ipsilateral hindlimb movement was observed at day 3 after SCI in any treatment group (BMS;0). However, BMS scoring in the NP

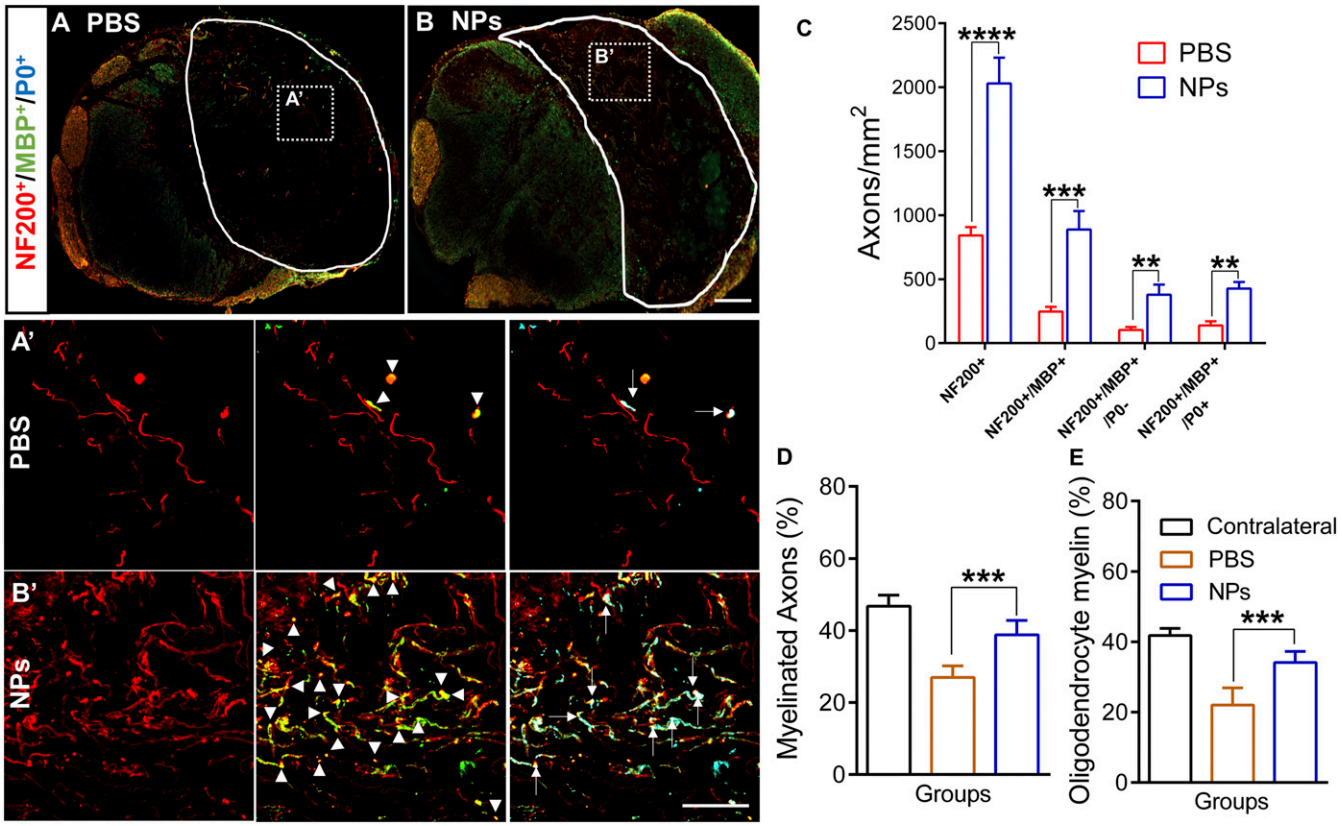

Fig. 4. NPs improve the axonal regrowth and remyelination in the chronic SCI phase. (*A* and *B*) Spinal cord sections were labeled using NF200 (axons), MBP (all myelination), and P0 (Schwann cells derived myelination) from PBS (*A*) and NP (*B*) conditions at the rostral location. The line indicated the bridge area for quantification and dashed line is for higher magnification area in *A′* and *B′*. White arrowheads show all myelinated axons ($NF200^+/MBP^+$), and white arrows indicate Schwann cell-derived myelinated axons ($NF200^+/MBP^+/P0^+$). (*C*) Quantification of total number of $NF200^+$, $NF200^+/MBP^+$, $NF200^+/MBP^+/P0^-$ (oligodendrocyte-mediated myelinated axons), and $NF200^+/MBP^+/P0^+$. (*D*) Proportion of axons that was myelinated within the bridge area. (*E*) Percentage of axons that was myelinated by oligodendrocytes. A 2-way ANOVA with Tukey's post hoc test for the multiple comparisons were performed where $^{**}P < 0.01$, $^{***}P < 0.001$, and $^{****}P < 0.0001$ relative to PBS group, mean ± SD, $n = 5$ per group. (Scale bars: *A* and *B*, 300 μm; *A′* and *B′*, 100 μm.)

group revealed a substantially improved locomotor function compared with the PBS group from day 7 through day 84 after SCI. In agreement with gene expression data, the BMS score in PBS group was significantly increased relative to the SCI-only group from day 70 after SCI, indicating that the bridge itself also has a positive effect on locomotor recovery. These data demonstrate that NPs have an early effect on reprogramming of circulating immune cells, which synergize with the microenvironment created by the bridge to induce long-term expression of RAGs at the injury, resulting in a proregenerative

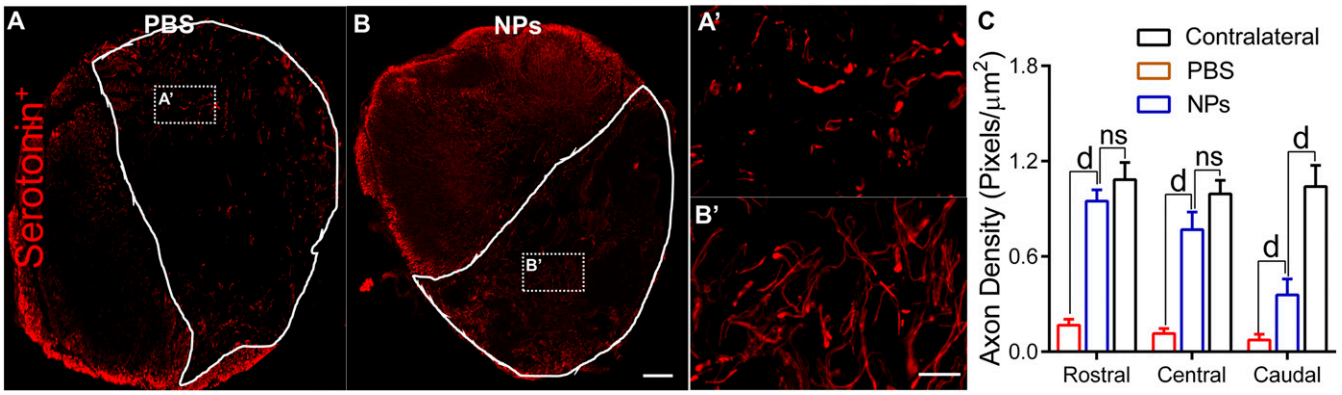

Fig. 5. Density of serotonergic fibers by NPs. (*A* and *B*) Spinal cord sections were labeled for serotonin from PBS (*A*) and NP (*B*) conditions at the rostral location in the chronic SCI phase. The line indicated the bridge area for quantification and dashed line is for higher magnification area in *A′* and *B′*. (*C*) Quantification of serotonergic axonal density in the bridge at rostral (0–400 μm), central (400–800 μm), and caudal (800–1,200 μm) locations from the rostral edge of the bridge/tissue interface. A 2-way ANOVA with Tukey's post hoc test for the multiple comparisons, where $^{d}P < 0.0001$ compared with PBS group, mean ± SD, $n = 5$ per group. (Scale bars: *A* and *B*, 300 μm; *A′* and *B′*, 100 μm.)

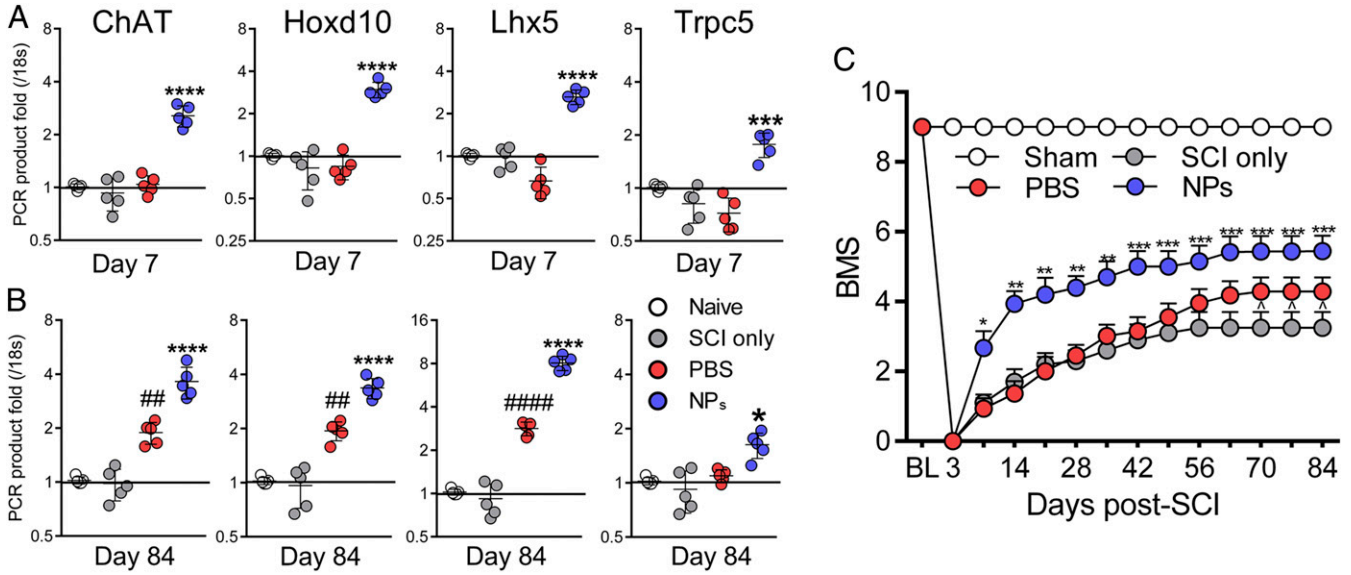

Fig. 6. Locomotor functional recovery by NPs. (*A* and *B*) Regeneration associated genes were investigated via qRT-PCR in the acute (*A*) and chronic (*B*) SCI phase. A one-way ANOVA with Tukey's post hoc test for the multiple comparisons, where $^{*}P < 0.05$, $^{***}P < 0.001$, and $^{****}P < 0.0001$ compared with PBS group, $^{\#\#}P < 0.01$ and $^{\#\#\#\#}P < 0.0001$ relative to SCI only, mean ± SD, $n = 5$ per group. (*C*) The ipsilateral hindlimb locomotor function was assessed using the BMS weekly for 84 d after SCI. NPs enhance the locomotor function following SCI. BL, baseline. A 2-way ANOVA with Tukey's post hoc test for the multiple comparisons, where, $^{*}P < 0.05$, $^{**}P < 0.01$, and $^{***}P < 0.001$, compared with PBS group and $\hat{}P < 0.05$ relative to SCI only, mean ± SD, $n = 18$ per group and time point.

microenvironment that is associated with an improved locomotor function after SCI.

Discussion

In the present study, we investigated the potential for reprogramming of circulating innate immune cells through NP administration to enhance functional regeneration following SCI. When innate immune cells are activated in the blood and spleen, they have high phagocytic capacity for scavenging apoptotic cells, cellular debris, and foreign invasive materials (24, 25). Generally, NPs may be perceived by inflammatory monocytes and neutrophils as foreign material and are then rapidly internalized (13, 26, 27). The rapid infiltration of various immune cells including inflammatory monocytes and neutrophils into the SCI leads to inflammatory response-derived secondary damage, contributing to further neuronal cell death, axonal dieback, demyelination, and scar tissue formation (4, 28). For in vivo SCI treatment, systemic depletion of immune cells has led to mixed results with some studies showing improved regeneration with partial depletion of select immune populations, while other studies show worsened histological and functional outcomes with complete depletion of certain immune populations (28). Herein, we focused on a nondepleting strategy targeting inflammatory cells in the vasculature, before their extravasation to the injury. We tested the hypothesis that particles could reprogram innate immune cell trafficking and phenotype to limit deleterious inflammatory responses, and promoting an environment that is a more permissive for regeneration.

i.v.-delivered NPs influence trafficking patterns of inflammatory monocytes and neutrophils, with a modest proportion of NP-positive cells trafficking to the spinal cord and the majority accumulating in the spleen. The spleen plays substantial roles in coordinating inflammatory responses and restoring immune homeostasis that lead to functional recovery after SCI (29). i.v.-administered NPs are thought to bind to circulating immune cells via scavenger receptors such as MARCO. NPs with a diameter of 500 nm were selected based on our previous work with autoimmune disease (30) and a greater internalization due in part to binding affinity for immune cells and flow patterns within the blood (12). Previous studies reported that neither resident microglia nor T lymphocytes express scavenger receptors such as MARCO (31), thus indicating that NPs target selectively circulating immune cells that would normally infiltrate a SCI. In agreement with previous studies, in vitro studies have demonstrated that NPs were internalized by bone marrow-derived macrophages (*SI Appendix*, Fig. S7) (12, 17). The sequestration of inflammatory monocytes/neutrophils in the spleen has been observed in other inflammation-mediated diseases models by NP treatment (12, 13, 15). In agreement with these previous studies, NPs reduced the number of inflammatory monocytes/neutrophils in the injured spinal cord, with this decrease likely indirectly decreasing tissue degeneration due to the reduced immune cell infiltration. However, we observed that NP-positive cells were present within the spinal cord, and our data suggest that these cells directly influenced the microenvironment by inducing a proregenerative phenotype that was more permissive for tissue regeneration. These results are also supported by gene expression analysis (*SI Appendix*, Fig. S5). In particular, both human and mice inflammatory monocytes express CCR2, which is principally responsible for recruitment and accumulation of these cells at inflammatory sites (12, 32). Previous study showed that delivery of CCR2 small interfering RNAs via liposome-reduced inflammatory monocyte trafficking in inflammatory disease models (32). However, because of widespread expression of CCR2 in other immune cells such as B cells and T cells, targeting CCR2 may have undesired side effects (33).

The cumulative effect of NP treatment is modulation of the microenvironment, which induces macrophage polarization from a proinflammatory phenotype toward a proregenerative phenotype. In the intact CNS, microglia/macrophages have both M1 and M2 properties; however, following SCI, proregenerative M2 macrophages are typically decreased, while pathological M1 phenotypes are increased and produce proinflammatory factors (21). Therefore, a transient and low number of M2 phenotype cells at the injury may fail to control secondary inflammatory events following primary SCI. NP treatment modulated the microenvironment and led to an M2-enhanced environment at the SCI site, with down-regulation of proinflammatory factors and

up-regulated expression of antiinflammatory factors such as Arg1, CD206, and IL-10 throughout day 84 after SCI. Interestingly, NP treatment also decreased the expression level of MCP-1, which is responsible for attracting circulating inflammatory monocytes to injuries by binding to its receptor CCR2 (12) and may also influence trafficking patterns of inflammatory monocytes after SCI. In addition, down-regulation of proinflammatory factors following NP treatment indicates that repeated-administration of NPs was well tolerated and reduced scar formation. Arg1 has been shown to promote wound healing and decrease the intensity and duration of inflammation (20). Similarly, CD206 and IL-10 both have demonstrated roles in modulating immune responses and secondary damage after injury. CD206 binds and removes apoptotic and necrotic cells without generation of cytotoxic byproducts after injury (21). The antiinflammatory cytokine IL-10 suppresses nuclear factor-κB (NF-κB) activation, leading to down-regulation of proinflammatory factors secretion (20). Consistent with these roles, NP treatment up-regulated the number of $CD206^+$ cells and M2 macrophages ($CD206^+/F4/80^+$) compared with the PBS group.

NP treatment significantly reduced both fibrotic and gliotic scarring after SCI. Lesion scarring represents both a mechanical and chemical impediment to axonal outgrowth and regeneration, and previous studies have demonstrated that macrophages lead to a profibrotic microenvironment by releasing proinflammatory factors. In both mice and human, these proinflammatory factors contribute to fibroblast activation and the induced secretion of connective tissue growth factor (CTGF) and collagen IV through SAMD2/3-mediated pathways, initiating formation of a dense, insoluble fibrotic matrix (34). Additionally, prior reports demonstrate that both circulating immune cells and hematogenous-derived macrophages recruit perivascular fibroblasts at the SCI, while depleting of hematogenous macrophages decreases the fibroblast accumulation and fibrotic scar area, enhancing axonal regrowth (35). In addition to fibrotic scarring, astrocytes also become reactive after SCI and are a major component of gliotic scarring. Reactive astrocytic responses are also initiated by proinflammatory factors that act through up-regulation of extracellular signal regulated kinase (ERK) signaling (8). In this study, NP inhibition of immune cell accumulation, induction of proregenerative phenotypes, and generation of antiinflammatory factors at the injury site may have altered fibroblast migration and astrocyte activation, reducing fibrotic and gliotic scarring and promoting axonal regeneration following SCI.

NP treatment has positive effects on axonal regeneration and remyelination after SCI. In the inflammatory microenvironment, proinflammatory factors are cytotoxic to neuronal cells and stimulate a short and arborizing growth pattern of axons after SCI (8, 21, 36). NP administration promotes axonal regrowth throughout the implanted-multichannel bridges compared with PBS injection. In the data reported herein, NP treatment influences the gene expression dynamics and macrophages polarization at the injury. Increased Arg1 by NPs at the injury enhances overexpression of polyamines, promoting cAMP downstream signaling pathway to activate axonal regrowth even in a myelin inhibitory microenvironment (21, 37). IL-10 has been reported to up-regulate expression of antiapoptotic factors and provide a direct trophic effect on axonal regeneration under the neurotoxic microenvironment (20, 38). CD206 promotes tissue remodeling after injury involving wound retraction and inflammatory resolution for tissue homeostasis (14). All of these factors may contribute to creating a proregenerative environment after SCI leading to axonal regeneration. Axonal remyelination after SCI is considered as a major component of the regenerative process and is mediated by multipotent oligodendrocytes progenitor cells (OPCs). Previous studies have indicated that macrophages polarization into proregenerative M2 phenotypes is an essential step for differentiation of OPCs for remyelination after SCI (20, 39). Moreover, an M2 mediated-regenerative factor activin-A directly binds to OPCs and facilitate OPC differentiation at the SCI (39, 40). Therefore, NP treatment-mediated reprogramming of innate immune cells toward proregenerative phenotypes may be a key component of the regenerative process for axonal regeneration and remyelination after SCI.

The early effects of NP treatment synergize with multichannel bridge to up-regulate long-term expression of RAGs and enhance functional recovery after SCI. PLG has been widely used for nerve tissues repair (8, 19, 41), with PLG biodegrading slowly into lactic and glycolic acid that are readily cleared from the tissue, metabolized, and eliminated from the body as carbon dioxide and water via citric acid cycle (42). Previously, we reported that bridge implantation alone increased the expression levels of axonal guidance-associated and synaptogenesis-associated gene ontologies at the SCI lesion (20), and altered the chemical balance and physical cues for a more permissive environment via infiltration of endogenous supportive cells, leading to release of factors for injury stabilization and attenuation of inflammatory responses (8, 19). Furthermore, mechanical guidance by the 3D structure of the bridge contributed to regeneration of descending axons and an increase in growth associated protein 43 (GAP-43) expression below the injury, leading to forelimb functional recovery (41). In addition, the bridge contributes to reducing the extent of scar formation and astrogliosis (8, 20). These characteristics of bridge implantation are consistent with the observed up-regulation of RAG expression and reduction of proinflammatory factors in our control group, which consisted of PBS injections in conjunction with bridge implantation. These results indicate that the bridge itself has the potential to support axonal regeneration via modest alteration of inflammatory responses and up-regulation of RAGs, leading to the locomotor functional recovery over the SCI-only group over time. BMS scores in the NP group were significantly increased starting from 1-wk after SCI compared with PBS, indicating that rapid NP-mediated inhibition of inflammatory immune cells accumulation led to less degeneration for rapid recovery of motor function. Furthermore, an improvement of locomotor skills was also observed from the PBS group at the chronic SCI phase compared with SCI only, which likely results from a more permissive environment enabling regeneration. These results were also supported by gene expression data. NP-derived immune cells modulation led to the long-term expression of multiple antiinflammatory factors and RAGs and induced a proregenerative environment at the injury. A number of genes associated with motor neurons were observed to be up-regulated at later time points. Choline acetyltranferase (ChAT), which marks mature motor neurons (43), had increased expression. Similarly, an increased expression of Homeobox D10 (Hoxd10) was observed, which organizes the patterning of motor neurons in the spinal cord (20). LIM homeobox 5 (Lhx5), implicated in the proliferation and differentiation of motor neurons (28), and transient receptor potential channel subfamily C (Trpc5), which leads to differentiation of neural progenitor cells (8, 9), were also up-regulated. Following SCI, descending serotonergic projections to spinal motor neurons were disrupted, leading to a decrease in serotonin levels and enhancing the locomotor dysfunction (22, 23). Our data demonstrate that NP treatment up-regulates the number of 5-HT fibers within bridges, which also may contribute to locomotor recovery. Taken together, these data demonstrate that NP treatment has early and rapid therapeutic impacts, which have long-term consequences with multichannel bridges synergistically, contributing to immune cells reprogramming toward proregenerative phenotypes. In addition, these effects lead to the long-term up-regulation of antiinflammatory factors, RAGs, and serotonergic fibers, promoting locomotor recovery after SCI.

In conclusion, this report demonstrates that NP treatment can modulate the inflammatory microenvironment after SCI. NP-mediated rapid reprogramming of innate immune cells has a sustained impact on microenvironment modulation at the SCI

injury when combined with bridge implantation. In addition, this regenerative microenvironment initiates a cascade of events, including induction of gene expression profiles associated with neural development and regeneration, which likely contributes to the enhanced numbers of regenerating and myelinated axons and improved functional recovery. Collectively, this strategy of targeting the innate immune cells in the vasculature before their extravasation to a SCI may have applications to other injury models associated with inflammation-mediated tissue damage. Furthermore, NPs are made of a Food and Drug Administration-approved material, stable at room temperature, do not contain an active pharmaceutical ingredient (API), and can be readily stored for immediate i.v. administration within the standard of therapy guidelines to limit secondary damage.

Materials and Methods

For additional methods, see *SI Appendix*.

Multichannel Bridges Fabrication. Initially, microspheres were fabricated using PLG [75:25 lactide:glycolide; inherent viscosity = 0.76 dL/g], then using a gas foaming and particulate leaching method, multichannel bridges were fabricated.

NP Fabrication and Injection. Cyanine 5.5 amine dye conjugated PLG (50:50, inherent viscosity = 0.55 dL/g) based particles were fabricated using an oil-in-water single emulsion solvent evaporation method. Each animal received 1 mg of particles (200 μL of suspension) via tail vein injection within 2 h after SCI per day for 7 d.

Animals. All animal surgery procedures and animal care were performed according to the Animal Care and Use Committee guideline at University of Michigan. C57/BL6 female mice (6–8 wk old, 20–25 g; The Jackson Laboratory) were used to create hemisection SCI model.

Functional Behavioral Test. Locomotor functional behavioral test was investigated using the open-field Basso Mouse Scale rating scale weekly until 12 wk after spinal cord injury.

ACKNOWLEDGMENTS. This study was supported by NIH Grants R01EB005678 and R01EB013198. We thank the Unit for Laboratory Animal Medicine at University of Michigan for animal care and maintenance.

1. J. Silver, J. H. Miller, Regeneration beyond the glial scar. *Nat. Rev. Neurosci.* **5**, 146–156 (2004).
2. G. Yiu, Z. He, Glial inhibition of CNS axon regeneration. *Nat. Rev. Neurosci.* **7**, 617–627 (2006).
3. J. Park *et al.*, Nerve regeneration following spinal cord injury using matrix metalloproteinase-sensitive, hyaluronic acid-based biomimetic hydrogel scaffold containing brain-derived neurotrophic factor. *J. Biomed. Mater. Res. A* **93**, 1091–1099 (2010).
4. D. J. Donnelly, P. G. Popovich, Inflammation and its role in neuroprotection, axonal regeneration and functional recovery after spinal cord injury. *Exp. Neurol.* **209**, 378–388 (2008).
5. M. R. Due *et al.*, Acrolein involvement in sensory and behavioral hypersensitivity following spinal cord injury in the rat. *J. Neurochem.* **128**, 776–786 (2014).
6. Z. Chen *et al.*, Mitigation of sensory and motor deficits by acrolein scavenger phenelzine in a rat model of spinal cord contusive injury. *J. Neurochem.* **138**, 328–338 (2016).
7. J. Park, B. Muratori, R. Shi, Acrolein as a novel therapeutic target for motor and sensory deficits in spinal cord injury. *Neural Regen. Res.* **9**, 677–683 (2014).
8. J. Park *et al.*, Reducing inflammation through delivery of lentivirus encoding for anti-inflammatory cytokines attenuates neuropathic pain after spinal cord injury. *J. Control. Release* **290**, 88–101 (2018).
9. J. Park *et al.*, Acrolein contributes to TRPA1 up-regulation in peripheral and central sensory hypersensitivity following spinal cord injury. *J. Neurochem.* **135**, 987–997 (2015).
10. J. Wang, Neutrophils in tissue injury and repair. *Cell Tissue Res.* **371**, 531–539 (2018).
11. D. R. Getts *et al.*, Microparticles bearing encephalitogenic peptides induce T-cell tolerance and ameliorate experimental autoimmune encephalomyelitis. *Nat. Biotechnol.* **30**, 1217–1224 (2012).
12. D. R. Getts *et al.*, Therapeutic inflammatory monocyte modulation using immune-modifying microparticles. *Sci. Transl. Med.* **6**, 219ra7 (2014).
13. D. R. Getts, L. D. Shea, S. D. Miller, N. J. King, Harnessing nanoparticles for immune modulation. *Trends Immunol.* **36**, 419–427 (2015).
14. J. C. Gensel, B. Zhang, Macrophage activation and its role in repair and pathology after spinal cord injury. *Brain Res.* **1619**, 1–11 (2015).
15. S. J. Jeong *et al.*, Intravenous immune-modifying nanoparticles as a therapy for spinal cord injury in mice. *Neurobiol. Dis.* **108**, 73–82 (2017).
16. C. L. Tsou *et al.*, Critical roles for CCR2 and MCP-3 in monocyte mobilization from bone marrow and recruitment to inflammatory sites. *J. Clin. Invest.* **117**, 902–909 (2007).
17. R. Kuo, E. Saito, S. D. Miller, L. D. Shea, Peptide-conjugated nanoparticles reduce positive co-stimulatory expression and T cell activity to induce tolerance. *Mol. Ther.* **25**, 1676–1685 (2017).
18. S. David, A. Kroner, Repertoire of microglial and macrophage responses after spinal cord injury. *Nat. Rev. Neurosci.* **12**, 388–399 (2011).
19. D. J. Margul *et al.*, Reducing neuroinflammation by delivery of IL-10 encoding lentivirus from multiple-channel bridges. *Bioeng. Transl. Med.* **1**, 136–148 (2016).
20. J. Park *et al.*, Local immunomodulation with anti-inflammatory cytokine-encoding lentivirus enhances functional recovery after spinal cord injury. *Mol. Ther.* **26**, 1756–1770 (2018).
21. K. A. Kigerl *et al.*, Identification of two distinct macrophage subsets with divergent effects causing either neurotoxicity or regeneration in the injured mouse spinal cord. *J. Neurosci.* **29**, 13435–13444 (2009).
22. M. Ghosh, D. D. Pearse, The role of the serotonergic system in locomotor recovery after spinal cord injury. *Front. Neural Circuits* **8**, 151 (2015).
23. B. J. Schmidt, L. M. Jordan, The role of serotonin in reflex modulation and locomotor rhythm production in the mammalian spinal cord. *Brain Res. Bull.* **53**, 689–710 (2000).
24. N. M. La-Beck, A. A. Gabizon, Nanoparticle interactions with the immune system: Clinical implications for liposome-based cancer chemotherapy. *Front. Immunol.* **8**, 416 (2017).
25. E. S. Kim, E. H. Ahn, T. Dvir, D. H. Kim, Emerging nanotechnology approaches in tissue engineering and regenerative medicine. *Int. J. Nanomedicine* **9** (suppl. 1), 1–5 (2014).
26. D. R. Getts *et al.*, Ly6c+ "inflammatory monocytes" are microglial precursors recruited in a pathogenic manner in West Nile virus encephalitis. *J. Exp. Med.* **205**, 2319–2337 (2008).
27. C. M. Dumont, J. Park, L. D. Shea, Controlled release strategies for modulating immune responses to promote tissue regeneration. *J. Control. Release* **219**, 155–166 (2015).
28. S. David, R. López-Vales, V. Wee Yong, Harmful and beneficial effects of inflammation after spinal cord injury: Potential therapeutic implications. *Handb. Clin. Neurol.* **109**, 485–502 (2012).
29. B. T. Noble, F. H. Brennan, P. G. Popovich, The spleen as a neuroimmune interface after spinal cord injury. *J. Neuroimmunol.* **321**, 1–11 (2018).
30. R. M. Pearson *et al.*, Controlled delivery of single or multiple antigens in tolerogenic nanoparticles using peptide-polymer bioconjugates. *Mol. Ther.* **25**, 1655–1664 (2017).
31. S. E. Hickman *et al.*, The microglial sensome revealed by direct RNA sequencing. *Nat. Neurosci.* **16**, 1896–1905 (2013).
32. F. Leuschner *et al.*, Therapeutic siRNA silencing in inflammatory monocytes in mice. *Nat. Biotechnol.* **29**, 1005–1010 (2011).
33. P. Boros, J. C. Ochando, S. H. Chen, J. S. Bromberg, Myeloid-derived suppressor cells: Natural regulators for transplant tolerance. *Hum. Immunol.* **71**, 1061–1066 (2010).
34. T. A. Wynn, L. Barron, Macrophages: Master regulators of inflammation and fibrosis. *Semin. Liver Dis.* **30**, 245–257 (2010).
35. Y. Zhu *et al.*, Hematogenous macrophage depletion reduces the fibrotic scar and increases axonal growth after spinal cord injury. *Neurobiol. Dis.* **74**, 114–125 (2015).
36. J. Park *et al.*, Neuroprotective role of hydralazine in rat spinal cord injury-attenuation of acrolein-mediated damage. *J. Neurochem.* **129**, 339–349 (2014).
37. D. Cai *et al.*, Arginase I and polyamines act downstream from cyclic AMP in overcoming inhibition of axonal growth MAG and myelin in vitro. *Neuron* **35**, 711–719 (2002).
38. Z. Zhou, X. Peng, R. Insolera, D. J. Fink, M. Mata, Interleukin-10 provides direct trophic support to neurons. *J. Neurochem.* **110**, 1617–1627 (2009).
39. V. E. Miron *et al.*, M2 microglia and macrophages drive oligodendrocyte differentiation during CNS remyelination. *Nat. Neurosci.* **16**, 1211–1218 (2013).
40. D. M. de Kretser, R. E. O'Hehir, C. L. Hardy, M. P. Hedger, The roles of activin A and its binding protein, follistatin, in inflammation and tissue repair. *Mol. Cell. Endocrinol.* **359**, 101–106 (2012).
41. K. Pawar *et al.*, Biomaterial bridges enable regeneration and re-entry of corticospinal tract axons into the caudal spinal cord after SCI: Association with recovery of forelimb function. *Biomaterials* **65**, 1–12 (2015).
42. H. K. Makadia, S. J. Siegel, Poly lactic-co-glycolic acid (PLGA) as biodegradable controlled drug delivery carrier. *Polymers (Basel)* **3**, 1377–1397 (2011).
43. Q. Yuan, H. Su, K. Chiu, Z. X. Lin, W. Wu, Assessment of the rate of spinal motor axon regeneration by choline acetyltransferase immunohistochemistry following sciatic nerve crush injury in mice. *J. Neurosurg.* **120**, 502–508 (2014).